Original Article

JCBFM

Journal of Cerebral Blood Flow & Metabolism
2019, Vol. 39(9) 1759–1775

DOI: 10.1177/0271678X18767748
journals.sagepub.com/home/jcbfm
SAGE

Hyaluronan impairs the barrier integrity of brain microvascular endothelial cells through a CD44-dependent pathway

Abraham J Al-Ahmad[1,2], Ronak Patel[2], Sean P Palecek[1] and Eric V Shusta[1]

Abstract

Hyaluronan (HA) constitutes the most abundant extracellular matrix component during brain development, only to become a minor component rapidly after birth and in adulthood to remain in specified regions. HA signaling has been associated with several neurological disorders, yet the impact of HA signaling at the blood–brain barrier (BBB) function remains undocumented. In this study, we investigated the impact of HA on BBB properties using human-induced pluripotent stem cell (iPSC) -derived and primary human and rat BMECs. The impact of HA signaling on developmental and mature BMECs was assessed by measuring changes in TEER, permeability, BMECs markers (GLUT1, tight junction proteins, P-gp) expression and localization, CD44 expression and hyaluronan levels. In general, HA treatment decreased barrier function and reduced P-gp activity with effects being more prominent upon treatment with oligomeric forms of HA (oHA). Such effects were exacerbated when applied during BMEC differentiation phase (considered as developmental BBB). We noted a hyaluronidase activity as well as an increase in CD44 expression during prolonged oxygen–glucose deprivation stress. Inhibition of HA signaling by antibody blockade of CD44 abrogated the detrimental effects of HA treatment. These results suggest the importance of HA signaling through CD44 on BBB properties.

Keywords

Blood–brain barrier, hyaluronan, permeability, stem cells, tight junctions

Received 7 July 2017; Revised 20 February 2018; Accepted 27 February 2018

Introduction

Hyaluronic acid (HA) is a linear glycosaminoglycan polymer chain formed by *N*-glucoronate-β1,4-*N*-acetyl-glucosamne dimers. HA can be divided into two groups based on their molecular weights: High-molecular weight HA (HA, >500 kDa) and low-molecular weight (oligomeric HA or oHA, <100 kDa). In the central nervous system, HA constitutes the main extracellular matrix component during mammalian brain development and rapidly decreases during early postnatal stages.[1–3] Such decrease in HA levels coincides with the maturation of the developmental blood–brain barrier (BBB).[4–6] In the adult CNS, HA localization is largely restricted to the perineural network. At the BBB, HA is located at the endothelial cell glycocalyx located on the luminal side.[7] Amongst the different putative HA receptors described in the literature,[8–10] CD44 appears as the main HA receptor expressed at the BBB. HA signaling has also been associated in various neurological diseases including fungal brain infection,[11,12] multiple sclerosis,[13–18] stroke,[19–21] suicidal depression,[22] and vascular dementia.[23] Yet, the biological effect of HA (and HA signaling) on the barrier function remains until now undocumented. Thus, we examined the effects of HA on BBB function using two complementary in vitro models, primary BMECs and iPSC-derived BMECs. Importantly, iPSC-derived BMECs are generated by differentiating human

[1]Department of Chemical and Biological Engineering, University of Wisconsin-Madison, Madison, WI, USA
[2]Department of Pharmaceutical Sciences, Texas Tech University Health Sciences Center, Amarillo, TX, USA

Corresponding author:
Abraham J Al-Ahmad, Department of Pharmaceutical Sciences, Texas Tech University Health Sciences Center, 1300 South Coulter Street, Amarillo, TX 79106, USA.
Email: abraham.al-ahmad@ttuhsc.edu

pluripotent stem cells as a mixture of neural and endothelial progenitors that gain BMEC properties in concert with key in vivo relevant signaling pathways including the canonical Wnt pathway,[24] such differentiation can be likened to a BBB "development" phase. After purification of the developing BMECs, they gain many properties of mature BMECs[24–27] and ultimately display a gene expression profile quasi-identical to primary or established human BMECs.[28,29]

Methods

Cell culture

Primary cultures and induced pluripotent stem cells used in this study were obtained and manipulated after protocols approval and by following the guidelines of the Institutional Biosafety Committee and the Animal Care and Use Committee of Texas Tech University Health Sciences Center and the University of Wisconsin–Madison, respectively. Human-induced pluripotent stem cells (iPSC-BMECs) were obtained from IMR90-c4 iPS cell line[30] (RRID:CVCL_C437) and differentiated using established protocols by Lippmann et al.[24] In brief, undifferentiated IMR90-c4 iPS colonies were maintained on growth-factor reduced (GFR) Matrigel (BD Biosciences, San Jose, CA, USA) in presence of mTeSR1 (Stem Cell Technologies, Vancouver, BC, Canada) for four days. BMECs differentiation was achieved by incubating such colonies for six days in presence of unconditioned media ((UM): DMEM/F12 15 mM HEPES (Thermofisher, Waltham, MA), 20% knockout serum replacement (Thermofisher), 1 × MEM non-essential aminoacids (Thermofisher), 1 mM Glutamax (Thermofisher), and 0.1 mM β-mercaptoethanol (Sigma-Aldrich, St. Louis, MO)). After six days of differentiation on UM, cells were allowed to mature into BMECs by incubating such cells for two days in presence of EC + (human endothelial serum-free medium (hESFM, Thermofisher), 1% platelet poor-derived bovine serum (PDS, Alfa-Aesar, Haverhill, MA) and 20 ng/mL basic fibroblast growth factor (bFGF, Bio-Techne, Minneapolis, MN)). After eight days of differentiation, cells were dissociated with accutase (Thermofisher) After eight days of differentiation, cells were enzymatically dissociated and seeded at a density of 10^6 cells/cm^2 on 12-wells polyester Transwells (0.4 μm pore size, Corning, Corning, NY, USA) coated with 80 μg/cm^2 collagen from human placenta (Sigma-Aldrich) and 20 μg/cm^2 fibronectin from bovine plasma (Sigma-Aldrich) and maintained in EC + for 24 h. After 24 h, cell medium was changed to EC− (EC medium supplemented with 1% PDS). Primary human brain microvascular endothelial cells (HBMECs) were purchased (Sciencell, Carlsbad, CA) and maintained as specified by the vendor, whereas rat brain microvascular endothelial cells (RBMECs) were isolated from adult Sprague-Dawley rats and maintained as previously described.[31,32] In brief, RBMECs were seeded on 12-wells polyester membranes (0.4 μm) and maintained in RBMEC medium (DMEM, 20% PDS, 1 μg/mL heparin, 2 mM L-glutamine, 4 μg/mL puromycin). IMR90-derived astrocytes and neurons were obtained following differentiation protocols previously described by our group.[33] In this study, we maintained neural progenitor cells (NPCs) grown on GFR Matrigel (Corning) in neural differentiation medium (NDM) for 48 h in presence of HA or oHA at different concentrations. Differentiating neurons were grown on GFR Matrigel in presence of neuronal maturation medium (NMM) for seven days. In co-culture experiments, freshly isolated IMR90-BMECs were seeded on Transwell® inserts placed over 21-days old astrocyte co-cultures. BMECs were maintained in presence of EC + during the first 24 h, followed by medium change to EC− during the next 24 h. Astrocytes co-cultures medium was changed after BMECs seeding into fresh astrocytes medium and maintained as such for 48 h. BMECs monocultures containing EC+/EC− on the apical chamber and astrocytes medium in the bottom chamber served as control for assessing the barrier function.

Hyaluronan and hyaluronidase treatment

High-molecular weight hyaluronan (HA, > 950 kDa) and ultra-low-molecular weight HA (oHA, 4–8 kDa) were purchased from R&D Systems (Bio-Techne) and dissolved in complete media. HA (or oHA) were added either at Day 6 of differentiation (48 h incubation) or at Day 10 of differentiation (24 h incubation). In experiments involving Transwell inserts, HA and oHA were added at the same concentration in both the apical and basolateral chambers unless specified. Anti-CD44 treatment was performed in presence of rat anti-CD44 (IM7 clone, 1:100, BD Biosciences, San Jose, CA), and rat isotype IgG (BD Biosciences) was used as control. Antibodies were added in both apical and basolateral chambers. In some experiments, we added HA only in the basolateral at the desired concentration. Cells were treated in presence of 10 U/mL *Streptomyces* hyaluronidase (Sigma-Aldrich) either from day 6 to day 8 or from day 9 to day 10.

Cell count

Cells treated with HA or oHA from day 10 to day 11 were fixed in 100% methanol (Sigma) and stained with DAPI (Sigma) and observed under an inverted fluorescence microscope at a 100 × magnification

(Leica X, Leica Microsystems, Wetzlar, Germany). Cell nuclei were counted using ImageJ (ImageJ, NIH, Bethesda, MD). An average of five random fields per experiment was used for data analysis. Cells treated with HA or oHA from day 6 to day 8 were dissociated by accutase (Corning) seeded at 10^6 cells/cm^2 and maintained as previously described. At day 10, cells were dissociated with accutase and counted using 0.4% Trypan Blue (Sigma) exclusion staining assay and an hemocytometer. Following the average cell density obtained at this timepoint, we adjusted the Transwell® seeding density to 1.55 and 1.75×10^6 cells/insert for HA and oHA-treated cells, respectively.

Cell metabolic activity

Cells were exposed to CellTiter Aqueous 96 MTS reagent (Promega, Madison, WI) at a dilution of 1:20 and allowed to incubate for 2 h. Absorbance was read using an ELISA plate reader set at 490 nm. Absorbance from MTS-containing blank medium was subtracted from the sample absorbance. Cell metabolic activity was normalized against the average absorbance of control group.

Barrier function assessment

Transendothelial electrical resistance (TEER) was measured using an EVOHM STX2 electrode system (World Precision Instruments, Sarasota, FL). Such TEER values were referred as baseline values and used to normalize changes in TEER observed following treatment. After treatment, changes in barrier tightness were measured using both TEER and paracellular permeability using sodium fluorescein using previously published protocols.[24,27] Baseline TEER and permeability values for all three BMECs under resting conditions can be found in Supplementary Table S1.

Immunofluorescence

Cells were fixed 4% paraformaldehyde (PFA, Electron Microscopy Sciences, Thermofisher) or 100% cold methanol, followed by permeabilization with 0.2% Triton-X100 solution (Sigma) with the exception of extracellular CD44 (eCD44) staining. Fixed cells were blocked in PBS with 10% normal goat serum (Sigma) for 1 h. Cells were incubated overnight with primary antibodies overnight at different concentrations (see Supplementary Table S2). Secondary antibodies (1:200, Life Technologies) were incubated for 1 h at room temperature and visualized with an inverted epifluorescence microscope (Olympus). Images were analyzed with ImageJ software (NIH, Bethesda, MD).

Alcian blue staining

Cells fixed with 100% cold methanol were treated with 3% acetic acid solution (pH 2.5) for 5 min followed by incubation with 5% Alcian Blue GX (Alfa-Aesar) dissolved in 3% acetic acid solution for 30 min followed by Nuclear Fast Red solution (Sigma-Aldrich) for 5 min. Images were acquired using an Olympus CK2 inverted tissue culture microscope and processed using ImageJ.

Flow cytometry

Dissociated cells were fixed, permeabilized and blocked as previously mentioned. Cells were incubated with primary and secondary antibodies as described in the previous section (Supplementary Table S2). Cells were washed with PBS containing 1% bovine serum albumin (Sigma) and sorted using a BD FACSCalibur (BD Biosciences). Flow cytometry data were analyzed using FlowJo X (FlowJo LLC, Ashland, OR). Mean fluorescence intensity from samples was subtracted from samples incubated with their respective IgG isotype controls.

Immunoblots

Cells were briefly washed with ice-cold PBS and incubated in presence of mammalian protein extraction reagent (M-PER, Thermofisher) for 10 min followed by a centrifugation at 14,000 r/min for 10 min at 4 °C. Cell lysate supernatants total protein content was assessed by BCA protein detection assay (Thermofisher); 20 µg of total protein was loaded in a 10% SDS-PAGE followed by a transfer on a nitrocellulose membrane (Bio-Rad, Hercules, CA) and incubation in presence of 1% BSA solution (Sigma). Membranes were probed overnight at RT in presence of mouse primary antibodies targeting β-actin (1:2000, Thermofisher), claudin-5 (1:500; Thermofisher), occludin (1:500, Thermofisher). Following incubation with primary antibodies, cells were washed with TBS-0.1% Tween 20 for 20 min each followed by incubation in HRP-conjugated secondary antibody (1:2000). Protein bands detection was achieved by incubation with enhanced chemiluminescent reagent (Pico West, Thermofisher), detected with X-ray films (Thermofisher) and digitally acquired using a Canon Pixma MX472 tabletop scanner (Canon Ltd). Images were processed using ImageJ (ImageJ, NIH, Bethesda, MD).

Hyaluronan ELISA

Acellular and cellular conditioned medium was collected and frozen at −80 °C until analysis. Samples were diluted by 1:1000 with ELISA diluent buffer and total hyaluronan concentration (HA≥35 kDa) was

assessed by (Bio-Techne). Samples concentrations were corrected for endogenous hyaluronan detected in complete medium.

P-glycoprotein activity assay

Cells were seeded at a density of 4×10^5 cells/cm^2 and allowed to recover in EC + for 24 h. Subsequently, these cells were incubated in EC + containing 10 μM Rhodamine 123 (Sigma) with or without 5 μM cyclosporine A (CsA, Sigma) for 1 h at 37 °C. Following such incubation, cells were washed with PBS and lyzed with 200 μl RIPA buffer (Thermofisher). Total fluorescence (RFU) was normalized to total protein content by BCA assay (Thermofisher).

Oxygen–glucose deprivation stress

Cells were incubated inside an hypoxic chamber (Biospherix, Laconia, NY) at 37 °C with an atmospheric gas mixture of 1% O_2, 5% CO_2 and 94% N_2 in glucose-free/pyruvate-free Dulbecco's Modified Eagle Medium (DMEM) supplemented with 1% PDS (DMEM-) for 24 h, as previously described by our group.[34] Cells maintained in DMEM containing 1 g/L glucose and 1% PDS served as normoxic control; 10 μM HA or oHA was added at the beginning of experiment only.

Statistics

Cells (including cell culture wells and inserts) were randomly assigned into each group through the experiment. Results were presented as mean ± S.D. from four independent experiments (each experiment was performed with two technical duplicates). Statistical analysis was performed using Graphpad Prism 7.0 statistical package (Graphpad Software, La Jolla, CA), using Students *t*-test (for comparison between acellular and cellular HA content) and one-way analysis of variance (ANOVA) supplemented by the Dunnett's post hoc test. $P<0.05$ was considered as statistically significant.

Results

High- and low-molecular weight hyaluronan impairs the barrier function in mature iPSC-derived BMECs

As high-molecular weight hyaluronan has been described as a barrier tightening extracellular matrix component (ECM) in the literature,[35–37] we investigated the presence of similar biological activity in our iPSC-derived BMECs by exposing mature (Day 10) iPSC-derived BMECs to high (HA; 960 kDa) and ultra-low (oHA; < 6.5 kDa) molecular weight hyaluronan (Figure 1(a)) at concentrations ranging from 0.1 to 10 μM. Such treatment had minimal impact on BMEC cell density and cell metabolic activity both following HA or oHA treatment (Figure 1(b) and (c)), with exception of 10 μM treatment. Next, we measured changes in the barrier function following HA or oHA treatment using TEER for up to 6 h (Figure 1(d) and (e)). We noted a biphasic response to HA in IMR90-derived BMECs, as noted by a decrease in TEER at 1 μM, but not at 0.1 μM and 10 μM (Figure 1(d)). Treatment with oHA resulted in a significant decrease in TEER at 0.1 μM (Figure 1(e)), but not at higher concentrations. Primary rat BMECs monocultures (RBMECs, Supplementary Figure 1(a)) showed a similar biphasic effect following HA treatment (maximum activity at 1 μM), yet all concentrations showed a decreased TEER. Next, we assessed the functional barrier outcome at 24 h timepoint (Figure 1(f) and (g)). We noted a decrease in TEER following HA treatment at concentrations as low as 0.1 μM; however, an increase in paracellular permeability (fluorescein) was significant only at 1 μM. Notably, oHA treatment failed to show a significant decrease in the barrier function at concentration below 10 μM. RBMECs showed a dose-dependent effect of HA on the barrier function, with a significant difference at 1 and 10 μM (Supplementary Figure 1(b) and (c)). Taken together, high-molecular weight hyaluronan exerted a detrimental effect on the barrier function via a dose-dependent mechanism.

Impact of HA and oHA on BMEC phenotype and HA signaling

We further investigated changes in BMEC phenotype by investigating changes in protein expression and localization following treatment with 10 μM HA or oHA (Figure 2), a concentration similar to values reported by Margolis et al.[3] in fetal rat brain. No major changes were observed in BMEC phenotype by immunofluorescence (Figure 2(a)). We noted a slight decrease in tight junction (TJ) immunoreactivity in both iPSC-derived BMECs (Figure 2(a)) and RBMECs (Supplementary Figure 1(e)), with only a significant decrease in ZO-1 protein levels (Figure 2(b)). We noted a clear decrease in CD44 immunoreactivity (Figure 2(c)) and protein levels (Supplementary Figure 2(a)) following hyaluronan treatment, as well as CD44$^+$ cells (Figure 2(d)). Expression of glycocalyx-associated hyaluronan in mature BMECs[7,38] appeared low, as we noted a fainted purple staining with no differences noted following HA and oHA treatment (Figure 2(e)). Nevertheless, we noted differences in P-gp activity following HA and oHA treatment in both iPSC-derived

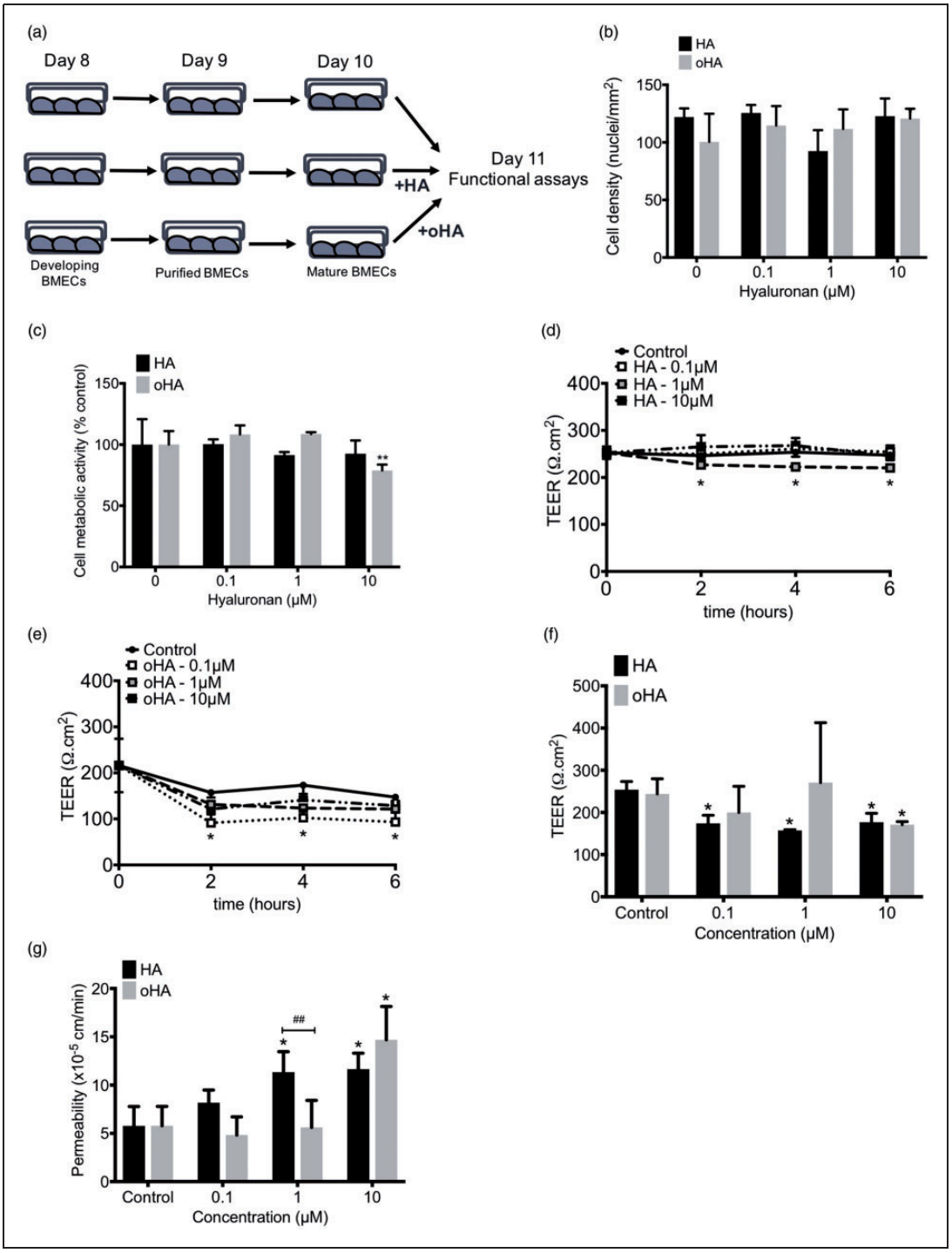

Figure 1. Hyaluronan impacts iPSC-derived BMEC monolayers barrier integrity via a dose-dependent manner.(a) Schematic representation of the hyaluronan treatment applied to mature iPSC-derived BMECs. At day 10, cells were treated with HA or oHA for 24 h. (b) Effect of HA and oHA treatment on BMEC cell density. Cell nuclei were counted using DAPI staining. (c) Cell metabolic activity following HA or oHA treatment. Dose-dependent effect of HA (d) and oHA (e) on iPSC-derived BMEC transendothelial electrical resistance following acute (<6 h) exposure. (f) Effect of prolonged (24 h) treatment on TEER. Note the difference in response between HA and oHA. (g) Fluorescein permeability in mature BMECs monolayers. Note the highest increase in permeability noted in iPSC-BMECs. * and ** denote $P < 0.05$ and $P < 0.01$ compared to control group, # denotes $P < 0.05$ between HA and oHA groups.

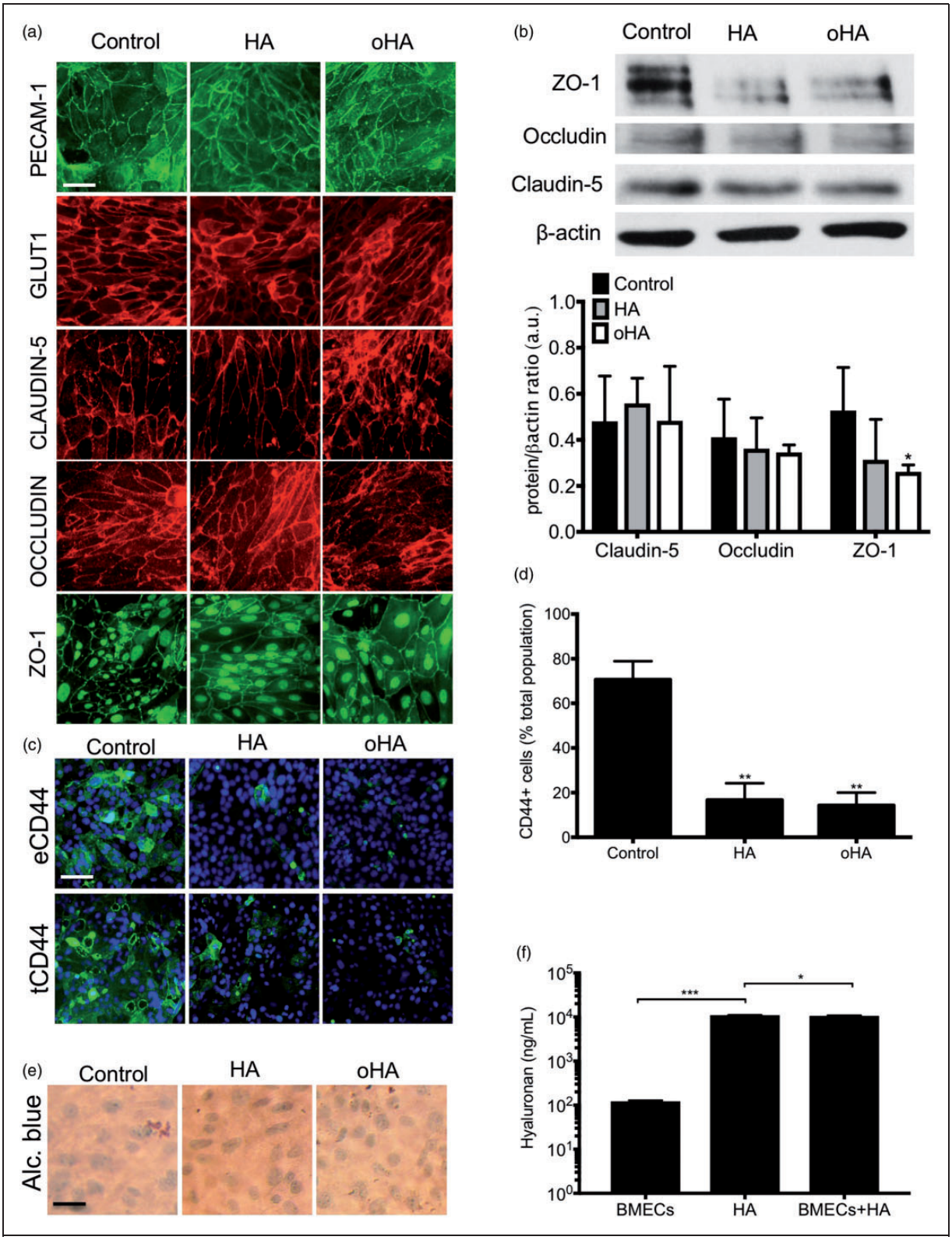

Figure 2. Hyaluronan treatment affects tight junction protein complexes and CD44 expression in mature iPSC-derived BMEC monolayers. (a) Representative immunocytochemistry pictures of mature BMECs (Day 11) following exposure to 10 μM HA or oHA. Note the partial detrimental effect of hyaluronan treatment on claudin-5 and occludin immunoreactivity. Scale bar = 30 μm. (b) Representative immunoblot for occludin and claudin-5 in iPSC-derived BMECs following HA or oHA treatment (top panel) and quantitative analysis (bottom panel). (c) Effect of hyaluronan treatment on CD44 expression and localization. Note the decrease in

BMECs and RBMECs (Supplementary Figure 1(e)), as CD44 interactions with HA and oHA can alter P-gp activity.[39] HA treatment partially induced P-gp activity (as measured by decrease in R123 uptake), whereas oHA treatment partially inhibited such activity in iPSC-derived BMECs. In contrast, RBMECs showed an inhibition with both HA and oHA.

Finally, we measured changes in HA levels (HA≥35 kDa) by ELISA (Figure 2(f)). We noted the presence of endogenous hyaluronan shedding in iPSC-derived BMECs, with an average concentration of 122.2 ± 5.46 ng/mL. In absence of BMECs, HA concentration was 10.98 ± 0.04 μg/mL, whereas such number decreased to 10.62 ± 0.23 μg/mL following incubation with BMECs. In conclusion, hyaluronan detrimental effect on the barrier function may be driven by the generation of HA degradation products from BMECs hyaluronidase activity.

CD44 inhibition blocks HA-mediated barrier disruption in mature BMECs

To assess the importance of the hyaluronan present in the cell glycocalyx, we investigated changes in the barrier function following treatment with a prolonged treatment with hyaluronidase (HAse) (Figure 3(a) and (b)). Notably, treatment with hyaluronidase resulted in an improved barrier function, as noted by an increase in TEER and decreased permeability. As we speculated that HA-mediated effects occur via CD44, we inhibited CD44 activity using IM7 (Figure 3), a CD44-shedding antibody.[40] Treatment of iPSC-BMECs with IM7 alone for 24 h from Day 10–11 increased TEER and decreased fluorescein permeability compared to IgG controls (Figure 3(c) and (d)). In addition, IM7 treatment abrogated HA and oHA-mediated activity on the barrier function. Treatment with IM7 also did not appear to substantially impact TJ complexes compared to IgG isotype control (Figure 5(e)), although we noted a decrease in $CD44^+$ cells following IM7 treatment (Figure 3(f)). Finally, IM7 partially inhibited P-gp activity as we noted a significant increase in R123 uptake compared to IgG (Figure 3(g)). In conclusion, HA and oHA-mediated effects on the barrier function appear mediated via a CD44-dependent mechanism.

Astrocytes co-cultures blunt HA-mediated effects on BMECs barrier function

Astrocytes play a significant function at the BBB, by inducing the barrier function in BMECs. Thus, we generated iPSC-derived astrocytes from the same iPSC line using our most recent protocol[33] and exposed astrocyte/BMECs co-cultures to HA (Figure 4(a) and (b)). Incubation of BMEC monocultures with astrocytes medium in the basolateral medium did not affect the BMEC barrier function (241 ± 160 $\Omega.cm^2$). Notably, presence of astrocytes blunted HA and oHA-mediated activity on the barrier function as we noted no differences in TEER and fluorescein permeability.

No differences were noted if hyaluronan was added to the basolateral chamber only (BL) or in both apical and basolateral (AP+BL). Astrocytes monocultures failed to show hyaluronan shedding activity (Supplementary Figure 2(a)), despite showing a partial hyaluronidase activity (10.68 ± 0.15 and 10.10 ± 0.10 μg/mL in HA alone or incubated with iPSC-derived astrocytes). In conclusion, astrocytes inhibit BMECs response to HA and oHA.

Oxygen–glucose deprivation stress impact CD44 expression in astrocytes and BMECs, but not HA degradation

Next, we investigated the effect of HA on prolonged oxygen–glucose deprivation stress in iPSC-derived BMECs (Figure 4(c) to (f)) following our published protocol.[34] Treatment with DMEM + under normoxia resulted in an absence of CD44 immunoreactivity (Figure 4(c)). However, OGD treatment resulted in an increased CD44 immunoreactivity (Figure 4(c)) that was further amplified following treatment with HA and oHA. We did notice an Alcian blue peri-nuclear purple staining in HA+OGD and oHA+OGD groups suggesting the presence of glycocalyx-associated hyaluronan. We did not notice an increase hyaluronan shedding or exogenous hyaluronan degradation following OGD stress (Figure 4(d)). Notably, treatment of OGD-BMECs with HA or oHA resulted in the partial maintenance of the barrier function both in TEER and permeability (Figure 4(e) and (f)). In conclusion, our

Figure 2. Continued
CD44 immunoreactivity in both the cell surface (eCD44) and total (tCD44). Scale bar = 30 μm (d) Quantification of $CD44^+$ cells. Total CD44 staining (tCD44) was used for quantification. (e) Alcian blue staining of iPSC-derived BMECs. Note the pale purple staining suggesting a low glycocalyx-associated hyaluronan. (f) Hyaluronan levels in BMECs without or with HA. Represented values were corrected against the endogenous hyaluronan content found in complete cell medium. Note the small but significant decrease in HA levels following incubation with BMECs compared to HA incubated in cell medium alone. * and ** denote $P < 0.05$ and $P < 0.01$ versus control group; # denotes $P < 0.05$ versus HA or oHA group.

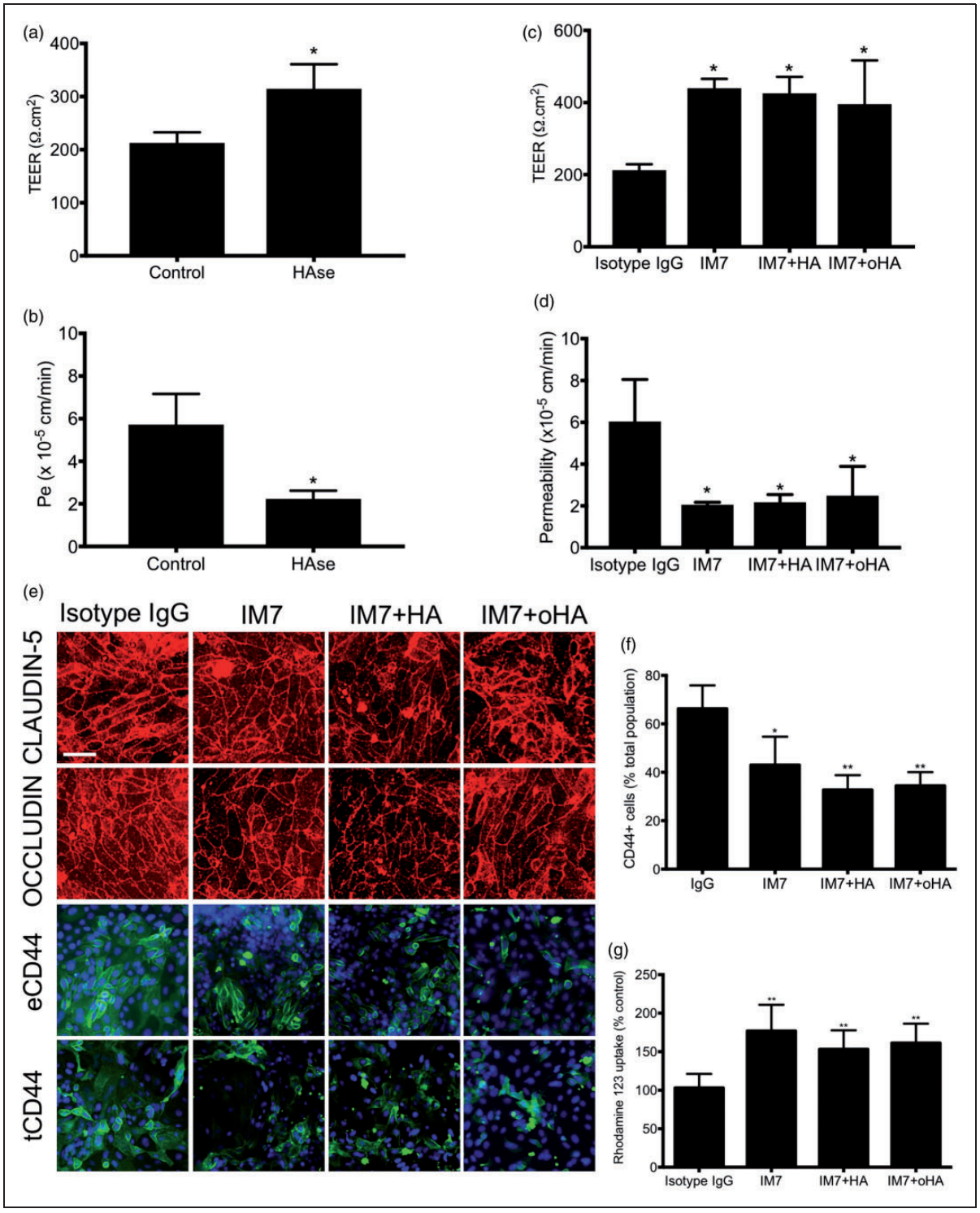

Figure 3. Removal of glycocalyx-associated hyaluronan or CD44 blockade by IM7 abrogates hyaluronan activity in mature iPS-BMECs. (a and b) Effect of hyaluronidase treatment on TEER and fluorescein permeability. Cells were treated with 100 U/mL hyaluronidase for 24 h. (c and d) Effect of IM7 on TEER and permeability. Cells were incubated in presence of IgG isotype or IM7 alone or in presence of HA or oHA for 24 h. (e) Representative immunocytochemistry pictures of mature iPSC-derived BMECs treated with IM7 with or without HA or oHA. Note the relative absence of change in TJ complexes and a decrease in total CD44 immunoreactivity. (f) Quantification of CD44-positive cells (tCD44), note a decrease following IM7. (g) IM7 inhibits P-gp activity, as noted by an increase in R123 uptake. * and ** denote $P < 0.05$ and $P < 0.01$ versus IgG isotype group, respectively.

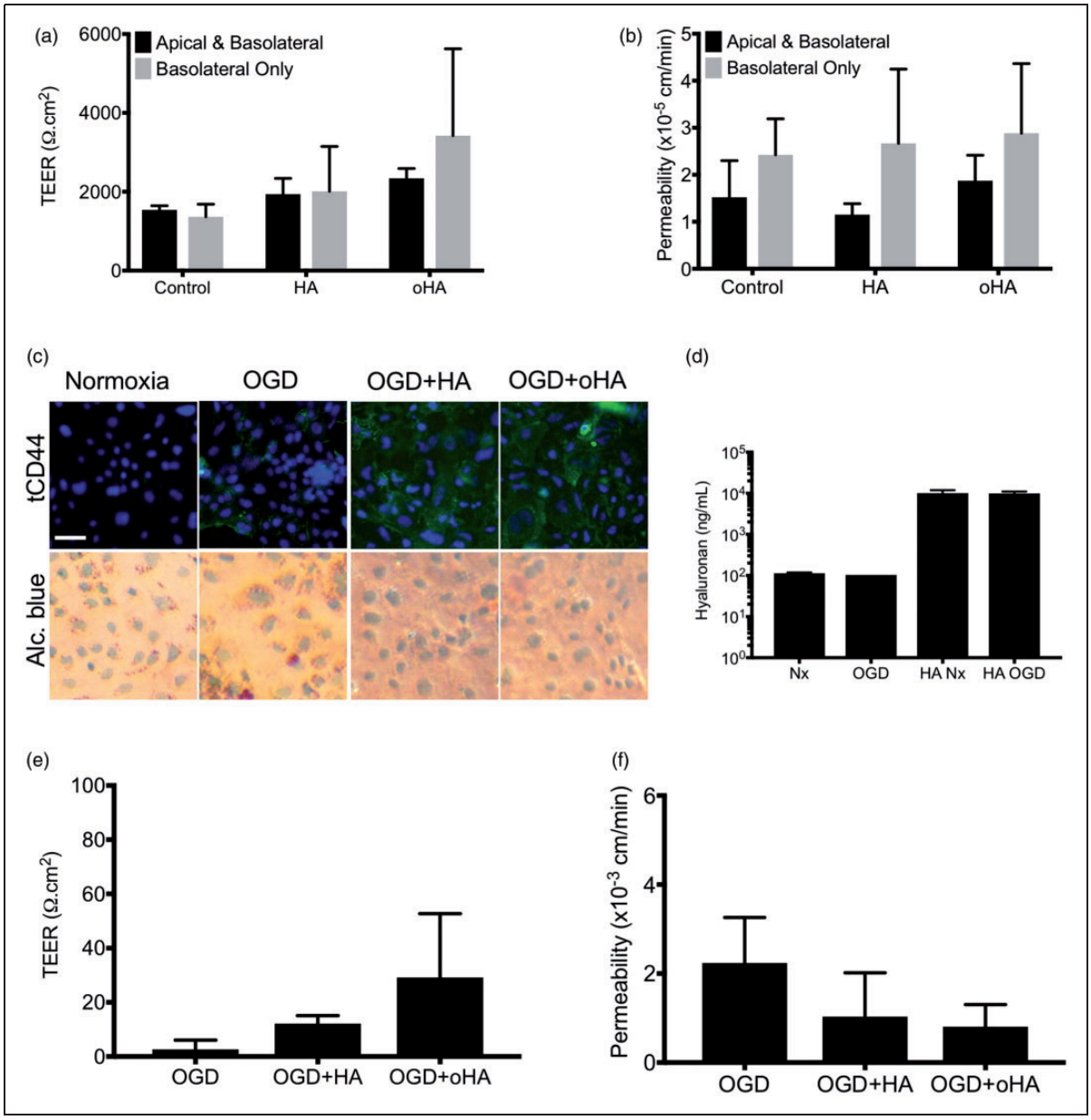

Figure 4. Impact of astrocytes and oxygen–glucose deprivation stress on hyaluronan biological activity. (a and b) TEER and fluorescein permeability values of astrocytes/BMECs co-cultures in presence of HA and oHA for 24 h. BMECs were co-cultured with astrocytes upon seeding at day 8 and maintained as monocultures; basolateral chamber was maintained in astrocytes medium. HA or oHA were added in both the apical and basolateral chamber (AP+BL) or basolateral chamber alone (BL). Note the absence of HA- or oHA-mediated effect on the barrier function, regardless of its location. (c) Expression of CD44 in IPSC-derived iPSC-derived BMECs during prolonged (24 h) OGD stress. Cells were exposed to oxygen–glucose deprivation stress (OGD, 1% oxygen and glucose-free DMEM/1% PDS) for 24 h in absence or presence of 10 μM HA or oHA. Note the absence of CD44 under normoxic condition in BMECs and its increase following OGD stress and concomitant presence of HA or oHA. (d) Hyaluronan levels following OGD stress. OGD stress has minimal effect on endogenous hyaluronan secretion. No differences in hyaluronan levels were observed following OGD treatment. (e and f) Impact of HA and oHA on the barrier function (TEER and fluorescein) during OGD stress. * denotes $P<0.05$ between HA incubated in acellular condition and HA incubated in presence of iPSC-derived astrocytes (astros).

data suggest the possible involvement of hyaluronan signaling during OGD stress.

Hyaluronan impairs BMEC yield

As we have demonstrated, astrocytes blunted HA-mediated activity on BMEC barrier function. Yet, astrocytes only appear in late stage of fetal brain development.[41] Barriergenesis occurs earlier during fetal brain development, encountering an hyaluronan-rich environment.[3,42–46] As our model display a cellular micro-environment similar to a developmental BBB (presence of neural progenitor cells (NPCs), endothelial cell differentiation and barriergenesis), we investigated the impact of HA and oHA treatment from Day 6 to Day 8 and measured changes in the barrier function at Day 9 (Figure 5(a)). Hyaluronan shedding by such BMECs/NPCs co-cultures (Figure 5(b)) was lower than mature BMECs (62.1 ± 0.89 ng/mL); however, we did not observe significant difference in HA degradation (10.98 ± 0.04 and 10.82 ± 0.39 μg/mL, respectively). Treatment with HA or oHA had minimal effects on BMEC phenotype ($PECAM1^+/GLUT1^+$) in differentiating BMEC colonies (Figure 5(c)). Treatment with HA and oHA increased cell density by Day 8 (Figure 5(d)); however, such proliferation was not present after purification as no changes in MTS were noted (Figure 5(e)). Noteworthy, HA and oHA partially decreased NPCs cell metabolic activity (Supplementary Figure 2(c)) and increased cell density (Supplementary Figure 2(d)) at concentrations lesser than 1 μM. Although we noted an important decrease in cell metabolic activity in neurons (Supplementary Figure 2(e)), we did not observe notable changes in $\beta III\text{-tubulin}^+$ neurites density (Supplementary Figure 2(f)).

Hyaluronan treatment during differentiation impairs BMEC barrier phenotype and function

Taking into account the difference in BMEC yield into BMECs Transwell filters seeding, we measured changes in the barrier function at Day 10 (Figure 5(g) and (h)). HA and oHA treatment had a lasting effect on the barrier function, as we noted lower outcomes in TEER and fluorescein permeability compared to control. The impact of HA and oHA was mostly visible on the BMEC phenotype at Day 9 (Figure 6), as we noted impaired TJ complexes in BMECs by immunofluorescence (Figure 6(a)) and immunoblots (Figure 6(b)). We noted a decrease in claudin-5 and ZO-1 immunoreactivity (Figure 6(a)) and protein levels (Figure 6(b)) and correlated with an increase in frayed junctions (Figure 6(c)). In addition to changes in TJ complexes, we noted a slight decrease in GLUT1 immunoreactivity (Figure 6(a)) and protein level (Supplementary Figure 2(b)) following hyaluronan treatment. As observed with mature BMECs, we noted a decrease in $CD44^+$ cells (Figure 6(e)) and CD44 protein levels (Supplementary Figure 3(c)). P-gp showed signs of delocalization (Figure 6(a)) and activity (Supplementary Figure 3(d)) but no changes in protein expression (Supplementary Figure 3(e)).

CD44 inhibition during BMEC differentiation improved barrier phenotype in iPSC-derived BMECs and mitigated the effects of HA treatment

We investigated the impact of CD44 blocking by IM7 antibody on BMEC phenotype outcome (Figure 7). As observed with mature BMECs (Figure 3), treatment with IM7 increased BMECs barrier function by acting both on TEER and fluorescein (Figure 7(a) and (b)). IM7 treatment reduced the number of frayed TJ complexes and number of $CD44^+$ BMECs (Figure 7(d) and (e)). As expected, IM7 partially inhibited P-gp activity in IMR90-derived BMECs (Figure 7(f)). In conclusion, our data indicate that CD44 inhibition eliminates most effects driven by HA or oHA, although CD44 inhibition on its own also affects BBB phenotype.

Discussion

Hyaluronan signaling pathway has been associated with various neurological disorders,[11,15,19,22] yet the impact of such pathway on the BBB integrity remains poorly understood. In this study, we investigated the effect of high (HA) and ultra-low (oHA) weight hyaluronan on the barrier function using IMR90 iPSC-derived and primary brain microvascular endothelial cells (BMECs) during their developmental (Days 6 to 8) and mature stage (Days 10 to 11). We observed a biological activity at 10 μM for both HA and oHA, such concentration was within range of values reported by Margolis et al.[3] in fetal rat brain. Such levels were 4-fold higher than an adult rat brain. On the other hand, Delpech et al.[47] reported average HA concentrations in human fetal and adult (cortex) brains of 12.35 and 1.8 mg/g dry tissues, respectively.

Both HA and oHA resulted in a detrimental effect on the barrier function, as we noted decreased TEER, increased fluorescein permeability and frayed TJ complexes. Such effect was associated with a decrease in TJ proteins (claudin-5, occludin, ZO-1) as noted by immunoblots and immunocytochemistry.

Notably, a recent study by Tang et al.[48] noted an increase in HA plasma level in patients suffering from stroke injury. In particular, such study noted an unfavorable outcome in patients suffering from either acute ischemic stroke or intracerebral hemorrhage and displaying HA plasma levels higher than 500 ng/mL. Such findings support the possible association between

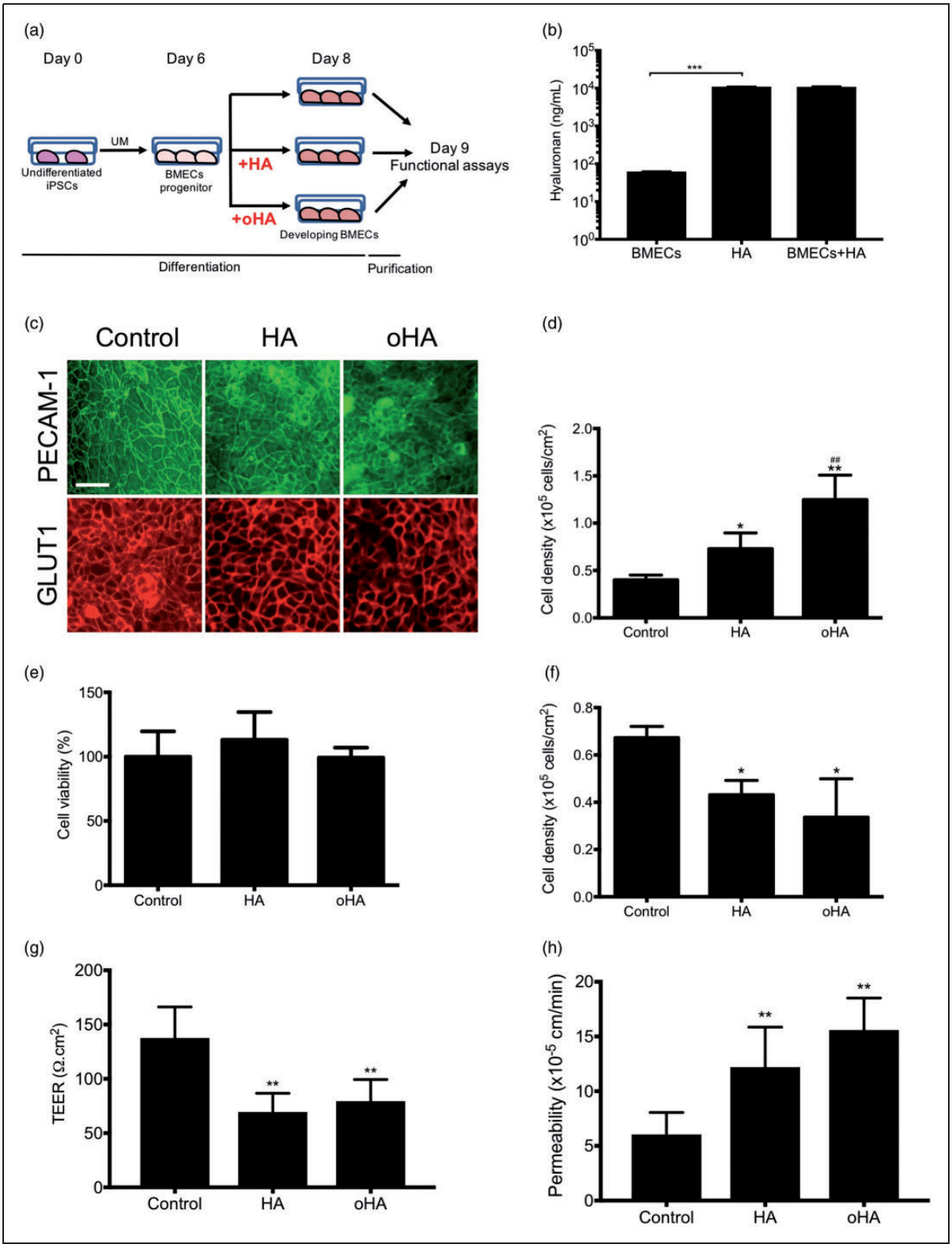

Figure 5. Hyaluronan treatment mildly affects iPSC-derived BMECs differentiation. (a) Schematic of the treatment of immature iPSC-derived BMECs with HA and oHA were treated with 10 μM HA or oHA from Day 6 to Day 8 of their differentiation. (b) Hyaluronan levels at day 8 of differentiation, in BMECs incubated without or with 10 μM HA. Hyaluronan level at day 8 (62.12 ± 0.89 ng/mL) was lower than observed at day 11 (122.2 ± 5.49 ng/mL). (c) Representative immunocytochemistry pictures of purified BMECs monolayers following HA and oHA treatment at day 8 of their differentiation, prior purification. BMECs colonies are

high HA levels and impaired BBB function. In our study, we have shown the increased permeability of BMECs monolayers following treatment with HA or oHA. The presence of similar response in vivo is yet to be documented; however, a recent study by Yao et al.[49] noted an increased Evans Blue permeability at the BBB following treatment with chitosan-based micro emulsions conjugated with HA. Similar outcomes were observed for paclitaxel using hyaluronan-conjugated nanoparticles.[50] Yet, such in vivo models failed to provide the mechanism of action of HA on the BBB that allow such increase in permeability. According to Lesley et al.,[51] CD44 affinity to HA is inversely proportional to the molecular weight, with high-molecular weight HA showing the highest affinity for CD44. A possible signaling pathway involved in hyaluronan-induced barrier disruption may involve small GTPases, including Rac1 and RhoA.[8] Both pathways appear important in the regulation of TJ integrity at the BBB,[52,53] thus we are further investigating how HA and oHA treatment are affecting such small GTPases.

In our study, HA and oHA displayed similar response. Hyaluronan ELISA data suggest the presence of an endogenous HA shedding and release in cell medium. Endogenous HA levels observed in our cell culture supernatants were similar to values observed in patients' plasma level.[48] In addition to endogenous HA production, we noted the presence of a hyaluronidase activity (via an hypothetical HYAL1 and HYAL2-mediated degradation) in our iPSC-derived BMECs capable to degrade exogenous hyaluronan. Yet, a limitation of this study is made by the limited discrimination of HA degradation byproducts. Such limitation was obvious in our OGD samples, as we did not observe significant differences in hyaluronan levels compared to normoxic samples. Therefore, we are currently investigating the possibility to refine our analytical method to quantify the nature of such HA degradation byproducts sorted by their size as well as assessing HYAL1 and HYAL2 in our cells during both normoxia and OGD stress, as such enzymes are reportedly up-regulated during stroke injury.[19]

Interestingly, CD44 appeared as the main receptor in HA-mediated activity on the BBB. We noted though that CD44 expression was decreased during the maturation process. In parallel, we also noted an increase in shed hyaluronan in iPSC-derived BMECs (but not in astrocytes). Such observation supports a study of Knudson et al.[54] pointing to an increased HA degradation following its binding with CD44. Furthermore, we noted up-regulation of CD44 expression during OGD stress in both iPSC-derived astrocytes and BMECs. CD44 has been recently described as a hypoxic responsive gene,[55] thus we are currently investigating the impact of OGD on CD44 expression. In addition, the presence of HA or oHA appeared to stabilize the barrier function, as we noted an increase in TEER and decrease in fluorescein permeability compared to cells treated with OGD only. In terms of developmental timing in vitro, hyaluronan treatment showed a more detrimental differentiating BBB compared to the mature BBB suggesting a crucial role of hyaluronan signaling in BBB development. Neural progenitor cells (NPCs) co-differentiating with BMECs have shown pivotal roles inducing a barrier phenotype, through signaling pathways such as Wnt/β-catenin and retinoic acid pathways.[24,27,56] We cannot exclude that the presence of HA or oHA may disrupt the maturation of both BMECs and NPCs during the time-window of our treatment (Day 6 to Day 8). Hyaluronan signaling appears an important pathway involved in NPC maintenance and differentiation in vivo.[57] Both HA and oHA affected IMR90-derived NPCs proliferation and metabolic activity, but showed no impact on neuronal differentiation and neurites outgrowth. Thus, it may be possible that the temporal regulation of hyaluronan during development may in part impact the timing of BBB development and maturation. Another effect noted in both primary and stem cell-derived BMECs is the effect of hyaluronan on P-gp activity. We observed an increase in P-gp activity (decreased R123 uptake) following treatment with HA, whereas oHA treatment resulted in a decrease of such activity. Moreover, treatment with IM7 also resulted in P-gp

Figure 5. Continued
characterized by the expression of both PECAM-1 and GLUT-1. Note the mild decrease in PECAM-1 immunoreactivity in oHA-treated groups. Scale bar = 30 μm. (d) Cell density analysis using Trypan blue exclusion assay. Cells were dissociated with accutase and counted using Trypan Blue. Note the increase in cell density at Day 8 following treatment with HA and oHA. (e) MTT assay was performed on cells freshly seeded at 1×10^5 cells/cm^2 and incubated for 4 h in presence of MTT reagent. MTT absorbance was adjusted to absorbance from blank (cell-free) well, absorbance values were normalized against control (untreated) cells. (f) Cell density count 24 h after seeding on collagen/fibronectin coated tissue culture plastic surface. All groups were seeded at a density of 1×10^5 cells/cm^2. Note the decrease in cell density following HA and oHA treatment suggesting a decrease in BMEC population. (g and h) TEER and fluorescein permeability values were obtained at Day 10. Note the increased permeability observed following HA and oHA treatment. iPSC-derived BMECs were treated with 10 μM HA or oHA from Day 6 to Day 8 of their differentiation. * and ** denote $P < 0.05$ and $P < 0.01$ compared to control group, # denotes $P < 0.05$ between HA and oHA groups.

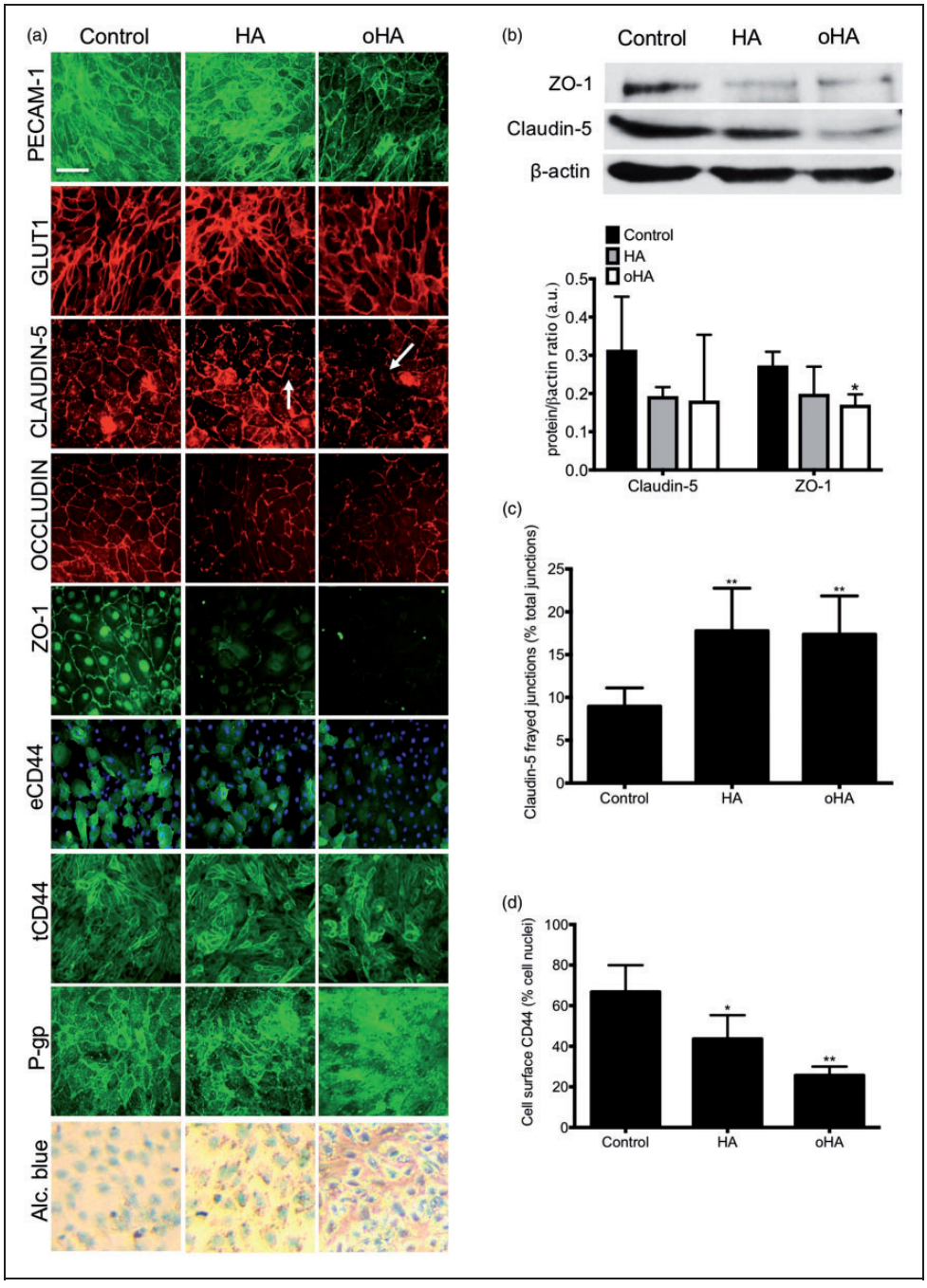

Figure 6. Hyaluronan treatment during BMECs differentiation impairs BMECs barrier function. (a) Representative micrograph pictures of confluent BMECs monolayers at Day 9. Note the presence of lacunar tight junction (TJ) complexes (claudin-5 and occludin) and decrease in ZO-1 immunoreactivity, indicative of frayed cell junctions (denoted by arrows). Note the decrease in extracellular CD44 (eCD44), but no differences in total CD44 (tCD44) were noted upon cell permeabilization with Triton-X100. Cell nuclei were counterstained using DAPI (blue). Also, note the changes in P-gp distribution in cells pre-treated with oHA. Scale bar = 30 μm. (b) Representative claudin-5 and ZO-1 immunoblots (top panel) and quantification (bottom panel) expression at day 9. Occludin bands were below detection levels. Note the decrease in claudin-5 and ZO-1 protein levels following hyaluronan treatment. (c) Quantification of frayed junctions in claudin-5 tight junction complexes. Cell junctions that did not display a smooth pattern or that was not visible was qualified as frayed junction. (d) Quantification of eCD44-positive cells at day 9. Note the decrease in eCD44-positive cells following HA and oHA treatment. * and ** denote $P < 0.05$ and $P < 0.01$ versus control group.

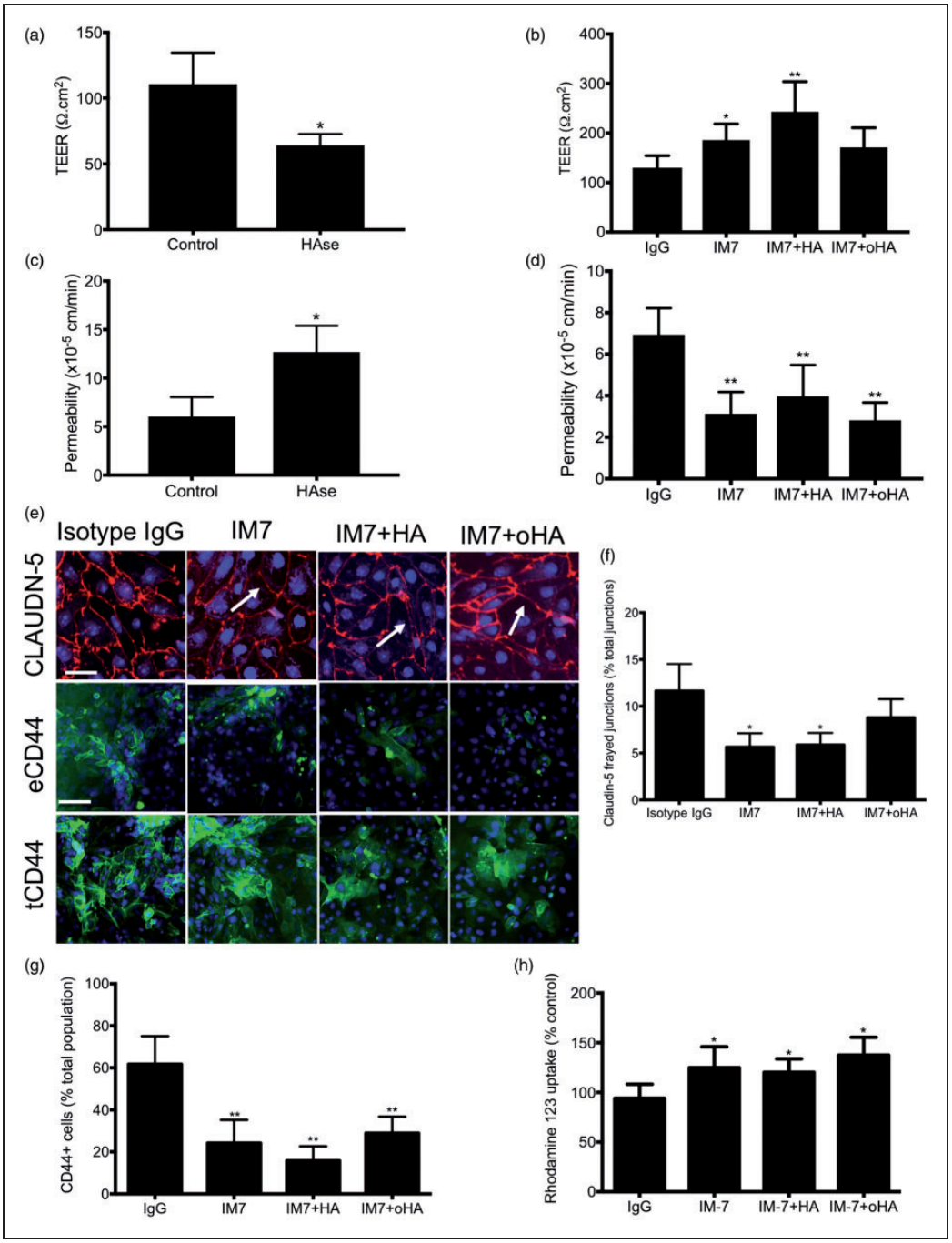

Figure 7. Exogenous hyaluronase treatment has a deleterious effect on BMEC maturation whereas CD44 blockade by IM7 reverses the detrimental effect of hyaluronan on BMEC differentiation. (a and b) Effect of hyaluronase treatment during the BMEC maturation phase on the barrier function. Cells were treated from Day 6 to Day 8 with bovine hyaluronidase (HAse; 100 U/mL), followed by purification on inserts. Cells were maintained in hyaluronidase-free medium from Day 8 to Day 9. TEER and permeability were measured at Day 9. Note the detrimental effect of HAse treatment on the barrier function, contrasting with its effect on mature BMECs. (c–h) Cells were incubated in presence of IM7 or IgG isotype concomitantly with HA or oHA during from Day 6 to Day 8. (c) TEER values obtained at Day 10. Note the intrinsic increase in TEER following treatment with IM7 alone or combined with hyaluronan treatment. (d) Fluorescein permeability at Day 10. Again, note the decreased permeability following treatment with IM7 alone or combined with hyaluronan treatment. (e) Representative micrograph picture of claudin-5, extracellular CD44 (eCD44) and total CD44 (tCD44) at Day 10 following treatment with IM7. Note the smoothening of claudin-5 TJ complexes (arrow) following treatment with IM7. (f) Quantification of frayed TJ complexes following IM7 treatment. Note the decrease by 50% of frayed junctions. (g) Quantification of tCD44-positive cells, as decrease in eCD44-positive cells was accompanied by a decrease in total number of cells expressing CD44 (eCD44 or tCD44). (h) CD44 blockade by IM7 partially inhibited P-gp activity up to 24 h after purification and abrogated the effect of HA and oHA P-gp activity. * and ** denote $P<0.05$ and $P<0.01$ versus IgG isotype control group.

inhibition. Such observation is in agreement with the existing literature, as expression and interaction of CD44 with P-gp have been associated with multidrug resistance in various cancer cell lines.[58–60] The mechanism of action of CD44-mediated P-gp activity in our model remains unclear; however, we speculate the contribution of the ezrin-radixin-moesin (ERM) complex-dependent pathway.[39] Taken together, this study emphasizes the deleterious effects of hyaluronan signaling on BBB integrity, and that such disruption occurred through a CD44-dependent pathway. Further study of hyaluronan signaling at the BBB is warranted as these data suggest a significant potential impact of hyaluronan on BBB health and disease.

Funding

The author(s) disclosed receipt of the following financial support for the research, authorship, and/or publication of this article: This project was supported by National Institutes of Health grant NS083688 to EVS and SPP and TTUHSC institutional funds to AA.

Acknowledgements

The authors would like to thank William Elmquist, James McCarthy and the late John Ohlfest for their helpful discussions.

Declaration of conflicting interests

The author(s) declared no potential conflicts of interest with respect to the research, authorship, and/or publication of this article.

Authors' contributions

AA, SPP and EVS designed, analyzed and interpreted the data. AA performed the experiments (RP performed the immunoblots). AA, SPP and EVS wrote the manuscript.

Supplementary material

Supplementary material for this paper can be found at the journal website: http://journals.sagepub.com/home/jcb

References

1. Preston M and Sherman LS. Neural stem cell niches: roles for the hyaluronan-based extracellular matrix. *Front Biosci* 2011; 3: 1165–1179.
2. Jones LL, Margolis RU and Tuszynski MH. The chondroitin sulfate proteoglycans neurocan, brevican, phosphacan, and versican are differentially regulated following spinal cord injury. *Exp Neurol* 2003; 182: 399–411.
3. Margolis RU, Margolis RK, Chang LB, et al. Glycosaminoglycans of brain during development. *Biochemistry* 1975; 14: 85–88.
4. Butt AM, Jones HC and Abbott NJ. Electrical resistance across the blood-brain barrier in anaesthetized rats: a developmental study. *J Physiol* 1990; 429: 47–62.
5. Keep RF, Ennis SR, Beer ME, et al. Developmental changes in blood-brain barrier potassium permeability in the rat: relation to brain growth. *J Physiol* 1995; 488(Pt 2): 439–448.
6. Kniesel U, Risau W and Wolburg H. Development of blood-brain barrier tight junctions in the rat cortex. *Brain Res Dev Brain Res* 1996; 96: 229–240.
7. Weinbaum S, Tarbell JM and Damiano ER. The structure and function of the endothelial glycocalyx layer. *Annu Rev Biomed Eng* 2007; 9: 121–167.
8. Singleton PA. Hyaluronan regulation of endothelial barrier function in cancer. *Adv Cancer Res* 2014; 123: 191–209.
9. Sloane JA, Batt C, Ma Y, et al. Hyaluronan blocks oligodendrocyte progenitor maturation and remyelination through TLR2. *Proc Natl Acad Sci USA* 2010; 107: 11555–11560.
10. Muto J, Yamasaki K, Taylor KR, et al. Engagement of CD44 by hyaluronan suppresses TLR4 signaling and the septic response to LPS. *Mol Immunol* 2009; 47: 449–456.
11. Jong A, Wu CH, Shackleford GM, et al. Involvement of human CD44 during Cryptococcus neoformans infection of brain microvascular endothelial cells. *Cell Microbiol* 2008; 10: 1313–1326.
12. Jong A, Wu CH, Gonzales-Gomez I, et al. Hyaluronic acid receptor CD44 deficiency is associated with decreased Cryptococcus neoformans brain infection. *J Biol Chem* 2012; 287: 15298–15306.
13. Brennan FR, O'Neill JK, Allen SJ, et al. CD44 is involved in selective leucocyte extravasation during inflammatory central nervous system disease. *Immunology* 1999; 98: 427–435.
14. Brocke S, Piercy C, Steinman L, et al. Antibodies to CD44 and integrin alpha4, but not L-selectin, prevent central nervous system inflammation and experimental encephalomyelitis by blocking secondary leukocyte recruitment. *Proc Natl Acad Sci USA* 1999; 96: 6896–6901.
15. Flynn KM, Michaud M, Canosa S, et al. CD44 regulates vascular endothelial barrier integrity via a PECAM-1 dependent mechanism. *Angiogenesis* 2013; 16: 689–705.
16. Flynn KM, Michaud M and Madri JA. CD44 deficiency contributes to enhanced experimental autoimmune encephalomyelitis: a role in immune cells and vascular cells of the blood-brain barrier. *Am J Pathol* 2013; 182: 1322–1336.
17. Katayama Y, Hidalgo A, Chang J, et al. CD44 is a physiological E-selectin ligand on neutrophils. *J Exp Med* 2005; 201: 1183–1189.
18. Winkler CW, Foster SC, Matsumoto SG, et al. Hyaluronan anchored to activated CD44 on central nervous system vascular endothelial cells promotes lymphocyte extravasation in experimental autoimmune encephalomyelitis. *J Biol Chem* 2012; 287: 33237–33251.
19. Al'Qteishat A, Gaffney J, Krupinski J, et al. Changes in hyaluronan production and metabolism following ischaemic stroke in man. *Brain* 2006; 129: 2158–2176.
20. Al Qteishat A, Gaffney JJ, Krupinski J, et al. Hyaluronan expression following middle cerebral artery occlusion in the rat. *Neuroreport* 2006; 17: 1111–1114.

21. Wang X, Xu L, Wang H, et al. CD44 deficiency in mice protects brain from cerebral ischemia injury. *J Neurochem* 2002; 83: 1172–1179.
22. Ventorp F, Barzilay R, Erhardt S, et al. The CD44 ligand hyaluronic acid is elevated in the cerebrospinal fluid of suicide attempters and is associated with increased blood-brain barrier permeability. *J Affect Disord* 2016; 193: 349–354.
23. Nagga K, Hansson O, van Westen D, et al. Increased levels of hyaluronic acid in cerebrospinal fluid in patients with vascular dementia. *J Alzheimers Dis* 2014; 42: 1435–1441.
24. Lippmann ES, Azarin SM, Kay JE, et al. Derivation of blood-brain barrier endothelial cells from human pluripotent stem cells. *Nat Biotechnol* 2012; 30: 783–791.
25. Canfield SG, Stebbins MJ, Morales BS, et al. An isogenic blood-brain barrier model comprising brain endothelial cells, astrocytes, and neurons derived from human induced pluripotent stem cells. *J Neurochem* 2017; 140: 874–888.
26. Wilson HK, Canfield SG, Hjortness MK, et al. Exploring the effects of cell seeding density on the differentiation of human pluripotent stem cells to brain microvascular endothelial cells. *Fluids Barriers CNS* 2015; 12: 13.
27. Lippmann ES, Al-Ahmad A, Azarin SM, et al. A retinoic acid-enhanced, multicellular human blood-brain barrier model derived from stem cell sources. *Sci Rep* 2014; 4: 4160.
28. Lim RG, Quan C, Reyes-Ortiz AM, et al. Huntington's disease iPSC-derived brain microvascular endothelial cells reveal WNT-mediated angiogenic and blood-brain barrier deficits. *Cell Rep* 2017; 19: 1365–1377.
29. Vatine GD, Al-Ahmad A, Barriga BK, et al. Modeling psychomotor retardation using iPSCs from MCT8-deficient patients indicates a prominent role for the blood-brain barrier. *Cell Stem Cell* 2017; 20: 831–843. e835.
30. Yu J, Vodyanik MA, Smuga-Otto K, et al. Induced pluripotent stem cell lines derived from human somatic cells. *Science* 2007; 318: 1917–1920.
31. Calabria AR, Weidenfeller C, Jones AR, et al. Puromycin-purified rat brain microvascular endothelial cell cultures exhibit improved barrier properties in response to glucocorticoid induction. *J Neurochem* 2006; 97: 922–933.
32. Lippmann ES, Weidenfeller C, Svendsen CN, et al. Blood-brain barrier modeling with co-cultured neural progenitor cell-derived astrocytes and neurons. *J Neurochem* 2011; 119: 507–520.
33. Patel R, Page S and Al-Ahmad AJ. Isogenic blood-brain barrier models based on patient-derived stem cells display inter-individual differences in cell maturation and functionality. *J Neurochem* 2017; 142: 74–88.
34. Page S, Munsell A and Al-Ahmad AJ. Cerebral hypoxia/ischemia selectively disrupts tight junctions complexes in stem cell-derived human brain microvascular endothelial cells. *Fluids Barriers CNS* 2016; 13: 16.
35. Lennon FE and Singleton PA. Hyaluronan regulation of vascular integrity. *Am J Cardiovasc Dis* 2011; 1: 200–213.
36. Bourguignon LY, Ramez M, Gilad E, et al. Hyaluronan-CD44 interaction stimulates keratinocyte differentiation, lamellar body formation/secretion, and permeability barrier homeostasis. *J Invest Dermatol* 2006; 126: 1356–1365.
37. Yokoi N, Komuro A, Nishida K, et al. Effectiveness of hyaluronan on corneal epithelial barrier function in dry eye. *Br J Ophthalmol* 1997; 81: 533–536.
38. Reitsma S, Slaaf DW, Vink H, et al. The endothelial glycocalyx: composition, functions, and visualization. *Pflugers Arch* 2007; 454: 345–359.
39. Zoller M. CD44: can a cancer-initiating cell profit from an abundantly expressed molecule? *Nat Rev Cancer* 2011; 11: 254–267.
40. Mikecz K, Dennis K, Shi M, et al. Modulation of hyaluronan receptor (CD44) function in vivo in a murine model of rheumatoid arthritis. *Arthritis Rheum* 1999; 42: 659–668.
41. Zerlin M and Goldman JE. Interactions between glial progenitors and blood vessels during early postnatal corticogenesis: blood vessel contact represents an early stage of astrocyte differentiation. *J Comp Neurol* 1997; 387: 537–546.
42. Delpech B, Delpech A, Bruckner G, et al. Hyaluronan and hyaluronectin in the nervous system. *Ciba Found Symp* 1989; 143: 208–220; discussion 221–232, 281–205.
43. Jenkins HG and Bachelard HS. Developmental and age-related changes in rat brain glycosaminoglycans. *J Neurochem* 1988; 51: 1634–1640.
44. Oohira A, Matsui F, Matsuda M, et al. Developmental change in the glycosaminoglycan composition of the rat brain. *J Neurochem* 1986; 47: 588–593.
45. Singh M, Chandrasekaran EV, Cherian R, et al. Isolation and characterization of glycosaminoglycans in brain of different species. *J Neurochem* 1969; 16: 1157–1162.
46. Singh M and Bachhawat BK. Isolation and characterization of glycosaminoglycans in human brain of different age groups. *J Neurochem* 1968; 15: 249–258.
47. Delpech B, Delpech A, Bruckner G, et al. Hyaluronan and Hyaluronectin in the Nervous System. In: Evered D and Whelan J (eds) *The biology of hyaluronan. Ciba Foundation Symposium 143*. Chichester, Sussex, UK: John Wiley & Sons, 1989.
48. Tang SC, Yeh SJ, Tsai LK, et al. Association between plasma levels of hyaluronic acid and functional outcome in acute stroke patients. *J Neuroinflammation* 2014; 11: 101.
49. Yao J, Zhou JP, Ping QN, et al. [Effect of hyaluronic acid chitosan-based microemulsion on the permeability of blood brain barrier in mice]. *Yao Xue Xue Bao* 2006; 41: 615–618.
50. Mittapalli RK, Liu X, Adkins CE, et al. Paclitaxel-hyaluronic nano-conjugates prolong overall survival in a preclinical brain metastases of breast cancer model. *Mol Cancer Ther* 2013; 12: 2389–2399.
51. Lesley J, Hascall VC, Tammi M, et al. Hyaluronan binding by cell surface CD44. *J Biol Chem* 2000; 275: 26967–26975.
52. Wang ZG, Cheng Y, Yu XC, et al. bFGF Protects against blood-brain barrier damage through junction protein regulation via PI3K-Akt-Rac1 pathway following

traumatic brain injury. *Mol Neurobiol* 2016; 53: 7298–7311.
53. Wu F, Chen Z, Tang C, et al. Acid fibroblast growth factor preserves blood-brain barrier integrity by activating the PI3K-Akt-Rac1 pathway and inhibiting RhoA following traumatic brain injury. *Am J Transl Res* 2017; 9: 910–925.
54. Knudson W, Chow G and Knudson CB. CD44-mediated uptake and degradation of hyaluronan. *Matrix Biol* 2002; 21: 15–23.
55. Yang M, Liu Y, Ren G, et al. Increased expression of surface CD44 in hypoxia-DCs skews helper T cells toward a Th2 polarization. *Sci Rep* 2015; 5: 13674.
56. Stebbins MJ, Lippmann ES, Faubion MG, et al. Activation of RARalpha, RARgamma, or RXRalpha increases barrier tightness in human induced pluripotent stem cell-derived brain endothelial cells. *Biotechnol J*. Epub ahead of print 28 September 2017. DOI: 10.1002/biot.201700093.
57. Su W, Foster SC, Xing R, et al. CD44 Transmembrane receptor and hyaluronan regulate adult hippocampal neural stem cell quiescence and differentiation. *J Biol Chem* 2017; 292: 4434–4445.
58. Miletti-Gonzalez KE, Chen S, Muthukumaran N, et al. The CD44 receptor interacts with P-glycoprotein to promote cell migration and invasion in cancer. *Cancer Res* 2005; 65: 6660–6667.
59. Hao J, Chen H, Madigan MC, et al. Co-expression of CD147 (EMMPRIN), CD44v3-10, MDR1 and monocarboxylate transporters is associated with prostate cancer drug resistance and progression. *Br J Cancer* 2010; 103: 1008–1018.
60. Chen H, Hao J, Wang L, et al. Coexpression of invasive markers (uPA, CD44) and multiple drug-resistance proteins (MDR1, MRP2) is correlated with epithelial ovarian cancer progression. *Br J Cancer* 2009; 101: 432–440.